

Microstructure and tribological properties of CrTiAlN composite coatings with high Cr content on 65Mn steels deposited by multi arc ion plating technology

Cai Zhihai Di Yuelan Zhang Ping

(National Key Laboratory for Remanufacturing, Academy of Armored Force Engineering, Beijing, 100072,

China)

Abstracts: The CrTiAlN composite coatings with different chemical composition are deposited on the surface of 65Mn steels by multi-ion plating technology in a gas mixture of Ar+N₂. The Metallic ratio of Cr, Ti, and Al was varied by adjusting the currents of different TiAl target. The coatings were characterized by means of energy dispersive X-ray(EDX) analysis, X-ray diffractometry(XRD), scanning electronic microscopy(SEM), microhardness tester, and ball-on-disc tribometer , respectively. The experimental results show that the surface morphology of CrAlTiN films are compact and dense. And the cross-section morphology appears as fibrous columnar crystals structure. Compared with CrN coatings, the preferential growth orientation of CrAlTiN films was changed from CrN (111) to CrN (200) after the addition of Ti, Al element. When the TiAl target arc current was 50A, the hardness reach the maximum value, 35GPa. The CrAlTiN composite films performs better than binary CrN as well as the Cr plating in teams of hardness and wear resistance at high temperature. Then the tribological mechanisms at high temperature for the above three kinds of coatings was discussed.

Key words: Ion plating, CrTiAlN composite coatings; Microstructure ; Tribological properties; Piston rings

1. Introduction

Functional hard chrome plating is a critical process associated with manufacturing and maintenance operations on aircraft , vehicles and ships, both in civilian and military sectors^[1,2]. Hard chrome electroplating is commercially used to produce wear-resistant coatings, but the plating bath contains hexavalent chromium, which has adverse health and environmental effects^[3,4]. For this reason, the use of hexavalent chromium will be limited. The types of coatings that are most widely viewed as being capable of replacing hard chrome plating are CrN based composite coatings. Compared with chrome electroplating, the CrN based composite coatings was one green manufacturing technologies, which appears high hardness, much more thermal stability and high-temperature wear resistant^[5,6].

In order to improve the life of piston rings, a multicomponent CrTiAlN composite coatings was synthesized by multi-arc ion plating technology. And the structural, mechanical, and tribological properties of CrTiAlN composite coatings with different chemical compositions were studied. Then the high-temperature wear resistant of chrome electroplating, CrN coatings and CrTiAlN composite coatings on the piston rings were compared.

2.Experimental Process

CrN and CrTiAlN composite coatings were deposited on 65Mn steel by using a multi arc ion plating system. The samples were mounted on the rotational substrate holder for the deposition of the CrTiAlN composite coatings. Chromium and Ti/Al (50/50 at.%) alloy targets were arranged on the two sides of the chamber. The average surface roughness (Ra) of the substrates was measured to be 0.015 μm by a surface profilometer. After

Corresponding author. Tel.: +86 10 66719249; fax: +86 10 66719249.

E-mail address: caizhihai2052@163.com

cleaning, the samples were installed into the deposition chamber and the system was pumped down into a high vacuum condition with a background pressure less than 4×10^{-3} Pa. The whole process of depositing CrTiAlN composite coatings is composed of such steps: ion cleaning for substrate, rendering with Cr coating, depositing Cr-CrN graded transition layer, depositing CrN-CrTiAlN interface transition layer, preparing CrTiAlN composite at last. The depositing condition of CrTiAlN composite coatings showed as follows: vacuum degree is less than 4×10^{-3} Pa, the depositing pressure is between $1 \sim 1.33 \times 10^{-1}$ Pa, the working temperature is about 300°C , the negative bias voltage of is -200 V , the deposition time is about 2h. And the contents of Cr, Ti, Al element are controlled by the ion current density ejected from the target. During the deposition course, the arc current of Cr target is keeping on 60 A. By adjusting TiAl target arc current from 0 A to 60 A, the CrTiAlN composite coatings with different composition were prepared. Table 1 summarizes the typical conditions for the synthesis of CrTiAlN coatings as well as their corresponding compositions.

Table 1 Deposition conditions for the synthesis of CrTiAlN coatings and their corresponding composition (in at.%)

Coatings systems	Target current (A)		Chemical compositions			
	I_{Cr}	I_{TiAl}	Cr	Ti	Al	N
CrN	60	0	50.4			49.6
CrTiAlN	60	40	36.7	8.7	4.5	50.1
	60	45	33.6	10.5	6.2	49.7
	60	50	29.2	11.9	8.5	50.4
	60	55	26.5	13.2	10.3	50.0
	60	60	24.8	14.5	11.2	49.5

The deposited samples were characterized for its compositional, structural, mechanical, and tribological properties. Elemental composition of the coatings was measured by energy dispersive X-ray (EDX) analysis. The chemical bonding states of the coatings were analyzed with X-ray photoelectron spectroscopy (XPS) scanning over an area of $1 \times 1 \text{ mm}^2$. The analysis was performed with a monochromatic Al $K\alpha$ X-ray source ($h\nu=1486.6\text{ eV}$). The nano-hardness and Young's modulus were measured by Nano Test 600 nano-sclerometer. The morphology and phase structure of the coatings for CrTiAlN composite coatings were analyzed by scanning electron microscopy (SEM, Quanta 200) and X-ray diffraction (XRD, Advance 8). The tribological behaviours of the coatings were studied by a ball-on-disc tribometer under oil sliding condition. The wear tests were carried out along a circular track of 8 mm diameter against a GCr15 ball at a linear speed of 0.20 ms^{-1} for 500m sliding distance at 200°C temperature. The tests were performed using an applied normal load of 5 N.

3. Results and discussion

3.1 Deposition velocity

Figure 1 shows the deposition velocity of CrTiAlN coatings with different TiAl target current. From Fig.1, it can be seen that the deposition velocity of CrTiAlN coatings increased with the increasing of TiAl target current. When the TiAl target current was 60A, the deposition velocity of CrTiAlN coatings reached maximum value, about 72 nm/min .

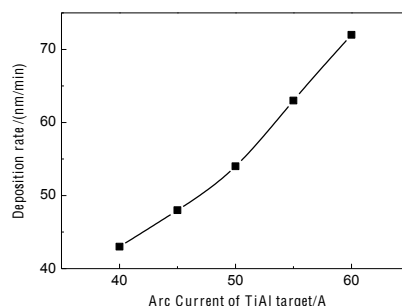


Fig.1 Deposition velocity of CrTiAlN coatings changing with TiAl target current

3.2 Compositional analysis

The elemental concentration of the deposited coatings was controlled by adjusting currents of the Cr and TiAl targets at a fixed substrate negative bias voltage. The compositions of the coatings were determined by EDX using the ZAF (Z: atomic number effect, A: absorption effect, F: fluorescence excitation effect) correction method. The relative error of this method was estimated to be less than 10%. In addition, the elemental concentrations of the coatings were also compared with the results determined by X-ray photoelectron spectroscopy (XPS). The XPS analysis was in accordance with the EDX results within $\pm 15\%$. In the EDX analysis (as shown in Table 1), ratios of metallic contents for Ti/(Cr+Ti+Al) and Al/(Cr+Ti+Al) increase monotonously up to 29 at.% and 22 at.%, respectively, with the increasing target currents (I_{TiAl}) from 0 to 60 A. Interestingly, the Ti content was found to be higher than the Al content when the target currents (I_{TiAl}) was varied with different number. This is associated with the different materials during reactive deposition in Ar/N₂ atmosphere. The metallic content ratio Cr/(Cr+Ti+Al), on the other hand, decreases from 100 to 49 at.% with the increasing addition of Ti and Al. The nitrogen content in all of the deposited samples is around 50 at.%. These results are basically consistent with XPS compositional analyses.

The chemical bonding structure of the coating samples was investigated by XPS. The typical spectra of the CrTiAlN coatings (prepared at $I_{\text{TiAl}}=60$ A) in Ti 2p, Cr 2p, Al 2p and N 1s energy regions before and after sputter etching are shown in Fig.2. It can be observed that each element of CrTiAlN coatings can be regarded as the superposition of several independent peaks with different binding energy. The N 1s spectra show only one main peak locating at 397.10 eV (Fig. 2a) is attributed to the presence of nitrides (e.g. Cr-N, Ti-N and Al-N)^[7]. deconvolution of the spectra indicates the presence of a second weak peak centred at 398.3 eV, which may be associated with the formation of chromium oxynitride. The Ti 2p_{3/2} and 2p_{1/2} broad peaks shown in Fig.2b are situated at positions at 455.2 eV and 461.3 eV, respectively, corresponding to the titanium nitride bonds. A complex structure between the doublet (456 eV-459 eV) can be reasonably attributed the presence of several reduced oxide phases such as Ti₂O₃ (456.8 eV) and TiO₂ (458.3 eV)^[8]. Deconvolution of Cr 2p_{3/2} peak indicates that it consists of three peaks centred at 575.7 eV, 576.6 eV and 578.6 eV (see Fig.2c) which can be due to the formation of CrN, Cr₂O₃ and CrO₂, respectively^[9]. The existing of CrO₂ peak and Cr₂O₃ peak indicate that some parts of coating surface have been oxidized after exposing in atmosphere. Peaks pertaining to free Cr metal (574.3 eV) and Cr₂N (574.5 eV) cannot be observed, indicating that the bonding state of chromium is in the form of CrN with traces of Cr-O compound. Similar to Cr element, the fitted Al 2p spectra can be analyzed to peaks of binding energy for 73.9 eV and 75.2 eV, which respond to Al-N bond and Al-O bond, besides, a small quantity of metal Al (72.3 eV) were also found (Fig.2d)^[10]. The analysis results indicate that Ti-N bond and Al-N bond are also existed in CrTiAlN coatings except for Cr-N bond after adding Ti, Al elements.

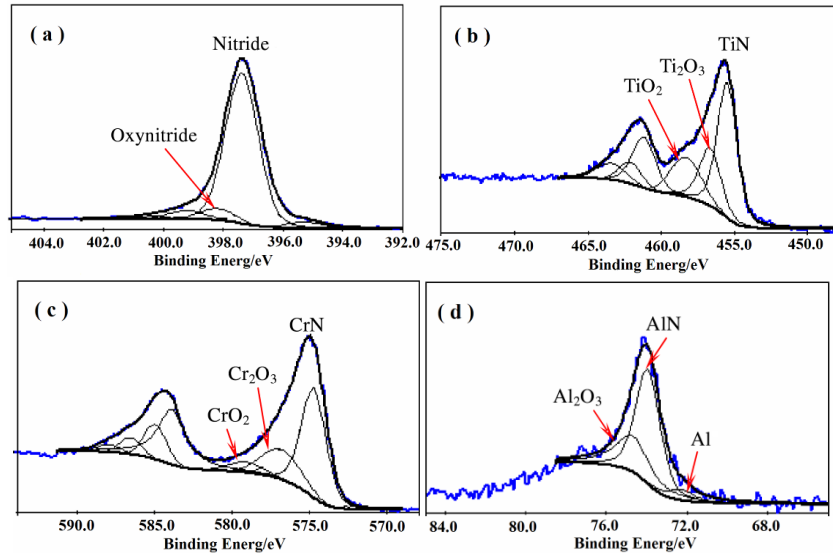


Fig.2 XPS spectra of CrTiAlN coatings (a) N1s (b) Ti2p (c) Cr2p (d) Al2p

3.3 Phase structure of CrTiAlN composite coatings

The XRD pattern of the Cr-Ti-Al-N coatings deposited under varying TiAl contents is shown in Fig.3. The pure CrN coating ($I_{TiAl}=0$) displays (111) and (200) diffraction peaks. With the increasing of Ti and Al additions, the CrN(200) peak exhibits a higher intensity comparing with other peaks, indicating the preferred orientation changes from (111) to (200). And it increased one weak broad diffraction corresponding to CrN(220) with increasing TiAl contents. The diffraction peak position of CrN(200) shifts slightly to lower angles from 2θ 43.69 to 43.31, when the target currents (I_{TiAl}) increase from 0 to 60A. The peak shift phenomenon may be related to the formation of TiN phase or the expansion of lattice. There is no evidence for the formation of Cr_2N phase in the deposited Cr-Ti-Al-N coatings, which is consistent with the XPS measurements. Therefore, Cr-Ti-Al-N coatings show the B1-NaCl (rock salt) structure^[11-13].

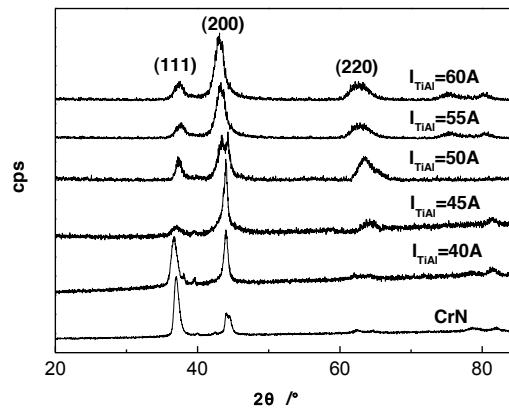


Fig.3 XRD analysis of CrTiAlN coating with different TiAl content

3.4 SEM analysis of CrTiAlN composite coatings

The surface morphology of CrN coatings and CrTiAlN coatings with different TiAl content are shown in Fig.4. It can be observed that the surface of CrTiAlN coatings was rougher than CrN coating, and the surface particles of coatings were increased and increscent with the increasing of TiAl content. According to TiAl duality phase diagram, $Ti_{50}Al_{50}$ corresponding to γ phase, whose maximal melting point was $1452^{\circ}C$ ^[14]. Compared with Cr target, the melting point of $Ti_{50}Al_{50}$ target was lower. And it is easy to vaporize bigger drop with ablation of

electric arc under high temperature, which makes particles size of CrTiAlN coatings increasing.

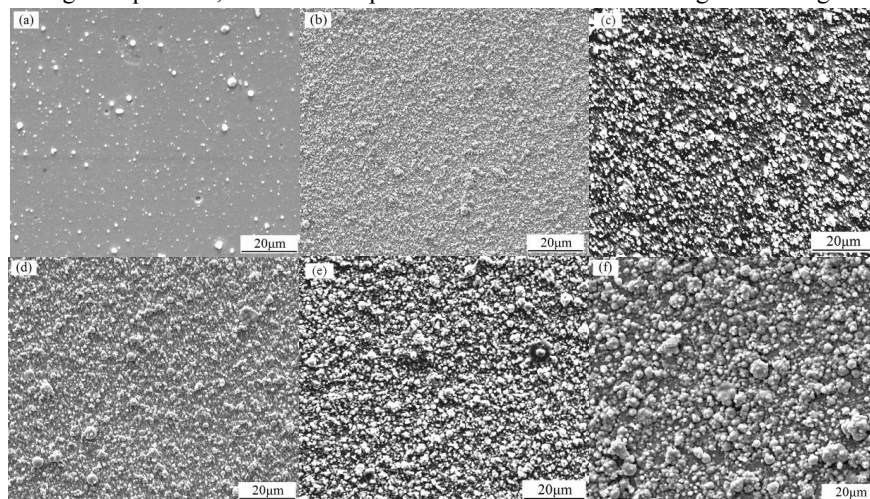


Fig.4 Surface morphology of $\text{Cr}_{1-x-y}\text{Ti}_x\text{Al}_y\text{N}$ coatings with different TiAl target currents , (a) $I_{\text{TiAl}}=0$, (b) $I_{\text{TiAl}}=40$,
(c) $I_{\text{TiAl}}=45$, (d) $I_{\text{TiAl}}=50$, (e) $I_{\text{TiAl}}=55$, (f) $I_{\text{TiAl}}=60$

Figure 5 is cross-section morphology analysis of CrTiAlN films when the TiAl target current was 50 A. From Fig.5, it can be seen that the structure of CrTiAlN films was column crystal. The column crystal structure of CrTiAlN films was grown uprightly from the interface. It was divided into two part in the cross-section morphology. The dark infrastructure was Cr/CrN transition region and the top white structure was CrTiAlN composite films.

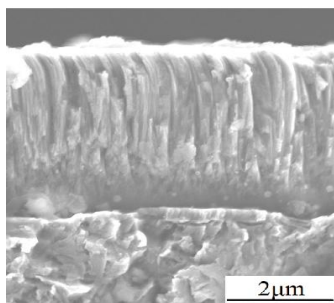


Fig.5 Cross-section morphology of CrTiAlN coatings

3.5 Hardness and Young's modulus of CrTiAlN coatings

Hardness and Young's modulus were measured as a function of indenter displacement using continuous stiffness measurement method. Figure 6 shows the value of hardness and Young's modulus under different TiAl content. From Fig.6, it can be seen that the hardness of $\text{Cr}_{1-x-y}\text{Ti}_x\text{Al}_y\text{N}$ coatings increased after the addition of Ti, Al element. The hardness of CrTiAlN coatings increased firstly, then reduced with the increasing of TiAl target arc current. When the TiAl target arc current was 50A, the hardness of CrTiAlN coatings reached the maximal value, 35GPa, which was higher than the Cr platings hardness 4.5 GPa and the CrN films hardness 22 GPa. The variation of Young's modulus for CrTiAlN coatings appears the same tendency with the increasing of TiAl content at the same time, which was accordant with hardness.

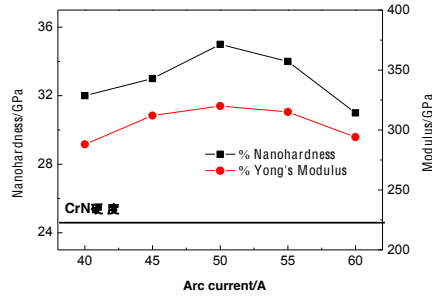


Fig.6 Hardness and Young's modulus of CrTiAlN coatings with different TiAl content

3.6 Tribological properties

Figure 7 shows the comparison of wear resistance with Cr, CrN and CrTiAlN ($I_{TiAl}=50$ A) coatings under oil lubrication condition at 200°C. From Fig.7a, it can be seen that the average friction coefficient of all samples falls in the range between 0.1 and 0.2. And the friction coefficient of Cr electroplating was higher than CrN coatings and CrTiAlN coatings. Among these three kinds coatings, the friction coefficient of CrTiAlN coatings was the lowest. It is noted that no direct correlation is found between the friction coefficient and the coating compositions. More stable friction coefficient during sliding is found for the quaternary CrTiAlN coatings as compared to Cr platings or CrN coatings. From Fig.6b, it can be seen that the lowest wear rate for CrTiAlN coatings can reach as low as $2.2 \times 10^{-4} \text{ mm}^3$, which is about 2.75 times lower than that of Cr plating. The wear volume sequence was as follows: Cr platings > CrN coatings > CrTiAlN coatings.

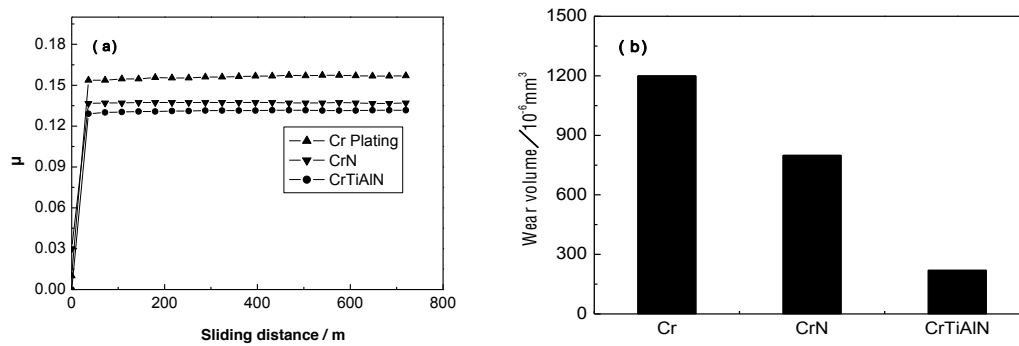


Fig.7 Comparison of wear resistance at high-temperature with different coatings

(a) friction coefficient with the sliding distance , (b) wear volume

Figure 8 shows the SEM images of the wear tracks for the Cr platings, CrN coatings, and CrTiAlN ($I_{TiAl}=50$ A) coatings after the wear tests under the same sliding conditions. Abrasive scratches are found on the surface for all the coatings, but less can be seen on the CrTiAlN surface (Fig.8c), indicating that abrasive wear might be the dominant mechanism in the sliding wear tests. It can be noted clearly that the surface was less worn or damaged for the quaternary CrTiAlN coating as compared to the others after the wear tests, which is associated with the wear rate measurements. While for Cr platings, it can be seen that the wear tracks of Cr platings was deep (Fig.8a). The surface layer of Cr platings has been peeled of seriously and plastic distortion has been happened heavily at the surface of wear tracks, which indicated oxidation abrasion was happened on the sliding process at high temperature. For CrN coatings, the wear tracks of CrN coatings was smooth, some small holes and shallow furrow scratches distributing on the surface layer (Fig.8b), whose wear mechanism was abrasive wear, too.

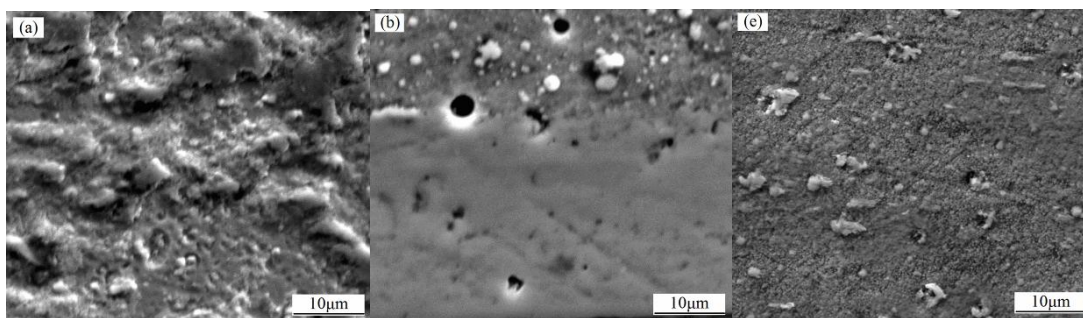


Fig.8 SEM pictures of the wear tracks after wear tests, (a) Cr plating , (b) CrN , (c) CrTiAlN

4. Conclusion

In this study, the multicomponent CrTiAlN composite coatings was synthesized by multi-arc ion plating technology. The experimental results show that the deposition velocity of CrTiAlN coatings increased with the increasing of TiAl target current. When the TiAl target current was 60A, the deposition velocity of CrTiAlN coatings reached maximum value, about 72nm/min. With the addition of Ti and Al elements, the resulting CrTiAlN coatings crystallize in the cubic B1-NaCl structure with a preferential growth orientation changing from CrN (111) to CrN (200). The metallic elements in the coatings react with nitrogen to form nitride phases such as CrN, TiN and AlN. No Cr₂N phase can be detected. The surface morphology of CrAlTiN films are compact and dense. And the cross-section morphology appears as fibrous columnar crystals structure. The optimised CrTiAlN hard coatings with hardness of 35 GPa are found to have superior wear performance at high-temperature as compared to Cr plating and CrN coatings. And the abrasive wear was the main wear mechanism. The specific wear rate can reach as low as $2.2 \times 10^{-4} \text{ mm}^3$, which is about 2.75 times lower than that of Cr electroplating. It is expected that these advantageous properties can enable the CrTiAlN coatings for a wide range of applications the surface of piston rings.

Acknowledgement

The financial support for this work by the National Natural Science Foundation of China (Project No. 50901089) is grateful acknowledged.

References

- [1] J. Vetter, G. Barbezat , J. Crummenauer , J. Avissar. Surface & Coatings Technology. 200 (2005) 1962.
- [2] Narendra B. Dahotre, S. Nayak. Surface & Coatings Technology. 194(2005) 58.
- [3] Carlos Eduardo Pinedo. Materials and Design. 24 (2003) 131.
- [4] J.A. Picas, A. Forn, G. Matthaus. Wear. 261 (2006) 477.
- [5] M. Uchid, N. Nihira. Surface and Coatings Technology. 177-178(2004)627.
- [6] P.L. Tam, Z.F. Zhou, P.W. Shum, K.Y. Li. Thin Solid Films. 516 (2008)5725.
- [7] C. Emery, A.R. Chourasia, P. Yashar, J. Electron Spectrosc. Relat. Phenom. 104 (1999) 91.
- [8] I. Bertoti, M. Mohai, J.L. Sullivan, S.O. Saied, Appl. Surf. Sci. 84 (1995)357.
- [9] A. Lippitz, T. Hubert, Surf. Coat. Technol. 200 (2005) 250.
- [10] S. Schoser, G. Brauchle, J. Forget, K. Kohlhof, T. Weber, J. Voigt, B.Rauschenbach, Surf. Coat. Technol. 103 (1998) 222.
- [11] H. Hasegawa, T. Yamamoto, T. Suzuki, K. Yamamoto, Surf. Coat. Technol. 200 (2006) 2864.
- [12] P.K. Ajikumar, A. Sankaran, R. Nithya, P. Shankar, S. Dash, A.K. Tyagi, B. Raj, Surf. Coat. Technol. 201 (2006) 102.
- [13] B. Warcholinski, A. Gilewicz, Z. Kuklinski, P. Myslinski. Vacuum. 83 (2009) 715.
- [14] S.G.Harris, E.D.doyle, A.C.Vlasveld et al. WEAR, 254(2003)723.